

# Global Levels of Specific Histone Modifications and an Epigenetic Gene Signature Predict Prostate Cancer Progression and Development

Tina Bianco-Miotto<sup>1</sup>, Karen Chiam<sup>1</sup>, Grant Buchanan<sup>1,2</sup>, Shalini Jindal<sup>1</sup>, Tanya K. Day<sup>1</sup>, Mervyn Thomas<sup>3</sup>, Marie A. Pickering<sup>1</sup>, Melissa A. O'Loughlin<sup>1,2</sup>, Natalie K. Ryan<sup>1</sup>, Wendy A. Raymond<sup>4</sup>, Lisa G. Horvath<sup>5,6</sup>, James G. Kench<sup>5,6</sup>, Phillip D. Stricker<sup>7,8</sup>, Willis R. Marshall<sup>9</sup>, Robert L. Sutherland<sup>6,8</sup>, Susan M. Henshall<sup>6,8</sup>, William L. Gerald<sup>10,†</sup>, Howard I. Scher<sup>11</sup>, Gail P. Risbridger<sup>12</sup>, Judith A. Clements<sup>13</sup>, Lisa M. Butler<sup>1</sup>, Wayne D. Tilley<sup>1</sup>, David J. Horsfall<sup>1</sup>, and Carmela Ricciardelli<sup>1,14</sup>; for the Australian Prostate Cancer BioResource

## Abstract

**Background:** Epigenetic alterations are common in prostate cancer, yet how these modifications contribute to carcinogenesis is poorly understood. We investigated whether specific histone modifications are prognostic for prostate cancer relapse, and whether the expression of epigenetic genes is altered in prostate tumorigenesis.

**Methods:** Global levels of histone H3 lysine-18 acetylation (H3K18Ac) and histone H3 lysine-4 dimethylation (H3K4diMe) were assessed immunohistochemically in a prostate cancer cohort of 279 cases. Epigenetic gene expression was investigated in silico by analysis of microarray data from 23 primary prostate cancers (8 with biochemical recurrence and 15 without) and 7 metastatic lesions.

**Results:** H3K18Ac and H3K4diMe are independent predictors of relapse-free survival, with high global levels associated with a 1.71-fold ( $P < 0.0001$ ) and 1.80-fold ( $P = 0.006$ ) increased risk of tumor recurrence, respectively. High levels of both histone modifications were associated with a 3-fold increased risk of relapse ( $P < 0.0001$ ). Epigenetic gene expression profiling identified a candidate gene signature (*DNMT3A*, *MBD4*, *MLL2*, *MLL3*, *NSD1*, and *SRCAP*), which significantly discriminated nonmalignant from prostate tumor tissue ( $P = 0.0063$ ) in an independent cohort.

**Conclusions:** This study has established the importance of histone modifications in predicting prostate cancer relapse and has identified an epigenetic gene signature associated with prostate tumorigenesis.

**Impact:** Our findings suggest that targeting the epigenetic enzymes specifically involved in a particular solid tumor may be a more effective approach. Moreover, testing for aberrant expression of epigenetic genes such as those identified in this study may be beneficial in predicting individual patient response to epigenetic therapies. *Cancer Epidemiol Biomarkers Prev*; 19(10); 2611–22. ©2010 AACR.

## Introduction

Epigenome alterations including DNA methylation and histone modifications contribute to cellular transformation and carcinogenesis (1, 2) and are characteristic of

most human malignancies. The most frequently studied epigenetic alteration in cancer is DNA methylation with global DNA hypomethylation being linked to activation of proto-oncogenes and chromosomal instability (3–5). Gene-specific DNA hypermethylation of promoter

**Authors' Affiliations:** <sup>1</sup>Dame Roma Mitchell Cancer Research Laboratories, Discipline of Medicine, <sup>2</sup>Molecular Ageing Laboratory, Freemasons Foundation Center for Men's Health, Discipline of Medicine, University of Adelaide and Hanson Institute, <sup>3</sup>Emphron Informatics, Brisbane, Queensland, Australia; <sup>4</sup>Flinders Medical Centre and Gribbles Pathology, Bedford Park, South Australia, Australia; <sup>5</sup>Sydney Cancer Centre, <sup>6</sup>Cancer Research Program, Garvan Institute of Medical Research, <sup>7</sup>Department of Urology, St. Vincent's Hospital, Darlinghurst, Sydney, New South Wales, Australia; <sup>8</sup>St. Vincent's Clinical School, Faculty of Medicine, University of New South Wales, Kensington, New South Wales, Australia; <sup>9</sup>Surgical and Specialty Services, Royal Adelaide Hospital <sup>10</sup>Department of Pathology, <sup>11</sup>Human Oncology and Pathogenesis Program, Memorial Sloan-Kettering Cancer Center, New York, New York; <sup>12</sup>Prostate and Breast Cancer Research Group, Department of Anatomy and Developmental Biology, Monash University, Clayton, Victoria, Australia; <sup>13</sup>Australian Prostate Cancer Research Centre-Queensland, Discipline of Molecular Biosciences and Institute of Health and Biomedical Innovation, Queensland University of

Technology, Kelvin Grove, Queensland, Australia; and <sup>14</sup>Discipline of Obstetrics and Gynaecology, School of Paediatrics and Reproductive Health, Research Centre for Reproductive Health, Robinson Institute, University of Adelaide, Adelaide, South Australia, Australia

**Note:** Supplementary data for this article are available at Cancer Epidemiology Biomarkers and Prevention Online (<http://cebp.aacrjournals.org/>).

T. Bianco-Miotto and K. Chiam contributed equally to this work.

† Deceased.

**Corresponding Author:** Carmela Ricciardelli, Discipline of Obstetrics and Gynaecology, School of Paediatrics and Reproductive Health, Research Centre for Reproductive Health, Robinson Institute, University of Adelaide, Adelaide, South Australia 5005, Australia. Phone: 618-8303-8255; Fax: 618-8303-4099. E-mail: [carmela.ricciardelli@adelaide.edu.au](mailto:carmela.ricciardelli@adelaide.edu.au)

doi: 10.1158/1055-9965.EPI-10-0555

©2010 American Association for Cancer Research.

regions is associated with the inactivation of genes involved in DNA repair, cell cycle regulation, apoptosis, and tumor suppression (6-8).

Histone modifications, such as lysine methylation and lysine acetylation, have been associated with clinical outcome in several cancers. Park et al. showed that high levels of H3K9triMe are associated with poor survival and that H3K9triMe is an independent prognostic factor in gastric adenocarcinoma (9). Barlesi et al. showed that immunohistochemical analysis for H2AK5Ac, H3K9Ac, and H3K4diMe could predict overall survival in non-small cell lung cancer (10). Others have shown that loss of H4K16Ac, H3K9triMe, H3K27triMe, and H4K20triMe is a common event in several cancers and can be used as prognostic markers (11-14). Mohamed et al. used the cellular levels of epigenetic modifications in the prostate to differentiate between benign and malignant disease (15), and recently it has been shown that DNA methylation decreases during disease progression (16), further supporting a role for epigenetic modifications in prostate carcinogenesis.

Recently, Seligson et al. (17) reported a relationship between global levels of several histone modifications and prostate tumor grade, but those specific histone modifications were not associated individually with tumor recurrence. A combination of at least two of the five assessed histone modifications (H3K18Ac and H3K4diMe), both associated with active transcription (18, 19), was required to predict tumor recurrence, but this was only observed in a subset of patients with low Gleason scores (17). Nevertheless, the findings of Seligson et al. (17) have not been replicated in a prostate cancer cohort with sufficient clinical follow-up and statistical power to establish the clinical relevance of histone modifications. Recently, H3K18Ac and H3K4diMe have been shown to predict clinical outcome in kidney and lung cancer (20). Therefore, in this study, we used immunostaining and quantitative image analysis to investigate whether H3K18Ac and H3K4diMe are predictive of tumor recurrence following radical prostatectomy in a large prostate cancer cohort with a long clinical follow-up (median, 9 years; refs. 21-25). We also investigated whether the expression of the genes encoding the enzymes involved in epigenetic modifications (i.e., epigenetic genes; ref. 26) are involved in prostate cancer development and progression.

## Materials and Methods

### Patient cohort

The St. Vincent's Hospital Campus Prostate Cancer Group (SVCPCG) tissue microarray (TMA) consisted of sections of arrayed prostate tissue replicate cores mounted on microscope slides. Samples of prostate tissue were collected from patients undergoing retropubic radical prostatectomy for clinically organ-confined prostate cancer ( $n = 279$ ) and each patient was represented in the TMA by at least duplicate 1-mm tissue cores (21). All tissue samples were surplus to diagnostic requirements and were obtained through the Garvan Institute

of Medical Research with approval from The University of Adelaide and the St. Vincent's Hospital (Sydney) Human Research Ethics Committees. Tumors were staged using the International Union against Cancer system (27). Prostate tumor recurrence was determined by prostate-specific antigen (PSA) failure, which was defined as a return to measurable serum PSA levels on two sequential measurements subsequent to a postoperative level below the sensitivity threshold of the assay ( $<0.2$  ng/mL). The clinical characteristics of the cohort are summarized in Supplementary Table S1.

### Immunodetection of H3K18Ac, H3K4diMe, and Ki67

Sections of paraffin-embedded prostate tissue (4  $\mu$ m) from the SVCPCG TMA cohort were immunostained with specific antibodies for H3K18Ac (rabbit polyclonal, ab1191; Abcam), H3K4diMe (rabbit polyclonal, ab7766; Abcam), and Ki67 (mouse monoclonal, M7240; Dako). The H3K18Ac and H3K4diMe antibodies used in this study have been previously utilized in similar immunohistochemistry studies (10, 17, 20, 28). These antibodies were optimized for our immunohistochemical protocol by performing serial dilutions for each antibody and ensuring that the antibody concentrations were within linear range. The optimal dilution chosen was one which retained specificity of staining without diminution of intensity. Tissue sections underwent microwave antigen retrieval (5 min, 750 W or 15 min, 350 W) in 10 mmol/L of citrate buffer (pH 6.5), and were incubated overnight with 1:7,500 H3K4diMe, 1:8,000 H3K18Ac, and 1:400 Ki67 dissolved in block (5% normal goat serum in PBS) at 4°C in a humidified chamber. Visualization of immunoreactivity was achieved using biotinylated antirabbit and antimouse immunoglobulins (1:400, 1 h, room temperature; Dako), streptavidin-peroxidase conjugate (1:500, 1 h, room temperature; Dako), and diaminobenzidine tetrahydrochloride to yield an insoluble brown deposit. A whole paraffin tissue section from a prostate cancer block known to be positive for the specified antigen was used as a positive control, and the primary antibody was omitted for the negative control.

### Quantitation of immunostaining

Cancer nuclei immunopositive for the proliferative marker Ki67 were scored visually by a pathologist (W.A. Raymond). Cancer nuclei immunopositive for H3K18Ac and H3K4diMe were independently scored by a pathologist (S. Jindal) and an experienced scientist (K. Chiam). All scorers were blinded to clinical outcome. H3K18Ac and H3K4diMe immunostaining was also quantified by using an automated video image analysis (VIA) system (VideoPro 32; Leading Edge P/L) as described previously (25, 29, 30). VIA measurements were confined to prostate cancer epithelial cells. Color images from contiguous fields for each tissue core were collected at a magnification of  $\times 400$ . VIA measurements included the diaminobenzidine tetrahydrochloride-stained area

(i.e., positively stained nuclear area in pixel units), the total nuclear area examined (i.e., positively and negatively stained nuclear area in pixel units), and the integrated optical density or absorbance (IOD) of diaminobenzidine tetrahydrochloride deposited in the cancer cells for each field. These values were used to derive three VIA measurements: (a) percentage of positive nuclear area (VIA positivity; % positive nuclear area), (b) mean IOD in positively stained nuclear area (MOD, intensity of nuclear staining), and (c) mean IOD in the total nuclear area examined (MIOD, total amount of staining).

### Microarray data analysis

Epigenetic genes which are defined as genes encoding enzymes involved in epigenetic modifications (26), were mined from a prior Affymetrix U95 microarray study done on manually dissected epithelial cells from 23 primary prostate cancer samples from radical prostatectomy patients with no therapy before surgery and 7 metastatic prostate cancer samples (31, 32). Eight of the 23 primary prostate cancer samples were from patients that experienced a biochemical recurrence. A heat map of the expression of the epigenetic genes in the prostate tumor samples was generated using Heatmap Builder version 1.0 (33).

### Epigenetic gene expression analysis by real-time quantitative PCR

RNA from 22 matched nonmalignant/tumor prostate samples from patients who had undergone retropubic radical prostatectomy was obtained from the Australian Prostate Cancer BioResource. The Gleason scores for the tumors were predominantly Gleason score 7 ( $n = 20$ ), one Gleason score 8, and one Gleason score 9. cDNA was synthesized from 300 ng of RNA using the iScript cDNA synthesis kit (Bio-Rad) according to the instructions of the manufacturer. Controls for the reverse transcription reaction included a "no RNA" control containing only the reverse transcriptase reaction mix, water, and enzyme; and a "RNA only" control that contained RNA template, water, and reverse transcriptase reaction mix, but no reverse transcriptase enzyme. cDNA was diluted 1:10 and 2  $\mu$ L was used in quantitative real-time PCR reactions which were done in triplicate in a total reaction volume of 20  $\mu$ L. TaqMan Gene Expression assays for *EZH2* (Hs01016789\_m1), *DNMT3A* (Hs01027166\_m1), *MBD4* (Hs00187498\_m1), *SRCAP* (Hs00198472\_m1), *MLL2* (Hs00231606\_m1), *MLL3* (Hs00407034\_m1), *NSD1* (Hs01076925\_m1), and the reference genes *GAPDH* (Hs99999905\_m1), *GUSB* (4333767F), and *HPRT1* (4333768F) were purchased from Applied Biosystems. cDNA was amplified using the TaqMan Gene Expression assays and TaqMan Gene Expression Master Mix (Applied Biosystems) on an iQ5 Cyclor (Bio-Rad) according to the instructions of the manufacturer. Reaction efficiency was determined using a standard curve from Universal Human Prostate RNA (Ambion) that had been reverse-transcribed and cDNA serially diluted to form the series 1:2, 1:10,

1:50, 1:250, and 1:1,250. Each standard was done in duplicate with 2  $\mu$ L per reaction and PCR products were visualized by agarose gel electrophoresis to confirm the size of the PCR products. The expression values for each of the epigenetic genes were normalized to an average of the three reference genes *GAPDH*, *GUSB*, and *HPRT1*.

### Statistical analysis

All analyses were done using SPSS 16.0 for Windows software (SPSS, Inc.). To evaluate the relationship with clinical outcome, H3K18Ac, H3K4diMe, and Ki67 levels were analyzed initially as continuous variables using univariate Cox regression analysis. Significant continuous variables were then analyzed as dichotomized values as outlined previously (34) and by ROC analysis (35). We found the greatest significance and highest specificity when a cutpoint of 6% positivity was used for Ki67, 50% positivity for H3K18Ac, and 30 MOD for H3K4diMe.

In Cox regression and Kaplan-Meier analyses, relapse-free survival was used as the end point to determine whether H3K18Ac, H3K4diMe, Ki67, or the histone score were related to risk of relapse. Relapse-free survival was calculated from the date of diagnosis to the date of relapse or the date of last follow-up if relapse-free. Spearman's correlation was used to determine correlations between H3K18Ac, Ki67, H3K4diMe, and clinicopathologic variables. Thirty-nine percent (109 of 279) of the patients had PSA failure at the time of census (December 31, 2006). Four patients who died from other causes were censored on the date of death. For the microarray data analysis, significant gene expression differences between the various groups were determined with a two-tailed Student's *t* test or Wilcoxon signed rank test for paired samples. Statistical analysis of the epigenetic gene signature by multivariate ANOVA was done using R version 2.9.1. Statistical significance for all analyses was set at  $P < 0.05$ .

## Results

### H3K4diMe, H3K18Ac and Ki67 immunostaining in prostate cancer

The majority of epithelial and stromal cell nuclei in the tumor regions of the TMA prostate tissue cores were positively immunostained for H3K18Ac and H3K4diMe (Fig. 1A and B). Positive immunostaining for both antigens was seen in the nonmalignant and prostate cancer cells (Supplementary Fig. S1). By visual assessment, the median H3K18Ac percentage of positive cancer cells was 97% (range, 7-100%) and for H3K4diMe was 95% (range, 9-100%). The Spearman correlation coefficients for the visual assessments between the pathologist and scientist was  $r = 0.935$  ( $P < 0.0001$ ) for H3K18Ac and  $r = 0.980$  ( $P < 0.0001$ ) for H3K4diMe. Immunostaining levels of H3K18Ac and H3K4diMe were also measured by VIA, which is an objective method of analysis (24, 25, 29). The three measures generated include VIA positivity (% positive nuclear area), intensity of staining

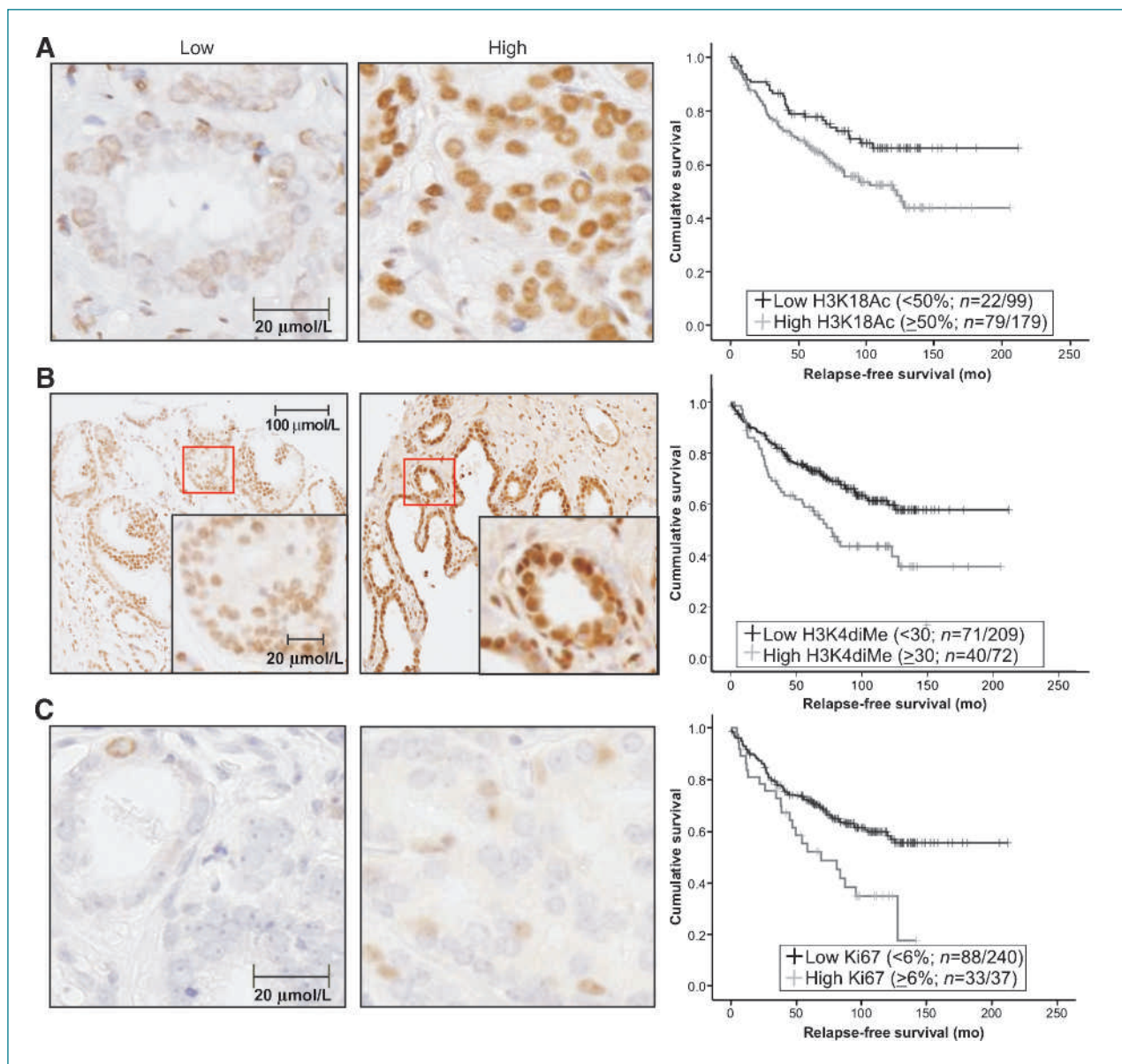


**Figure 1.** Immunostaining patterns and Kaplan-Meier product limit plots of relapse-free survival of H3K18Ac, H3K4diMe, and Ki67 in the prostate TMA samples. Images of prostate tumor tissue samples with low and high immunostaining for H3K18Ac (A; low positive nuclear area <50%, high positive nuclear area  $\geq$ 50%), H3K4diMe (B; low MOD intensity <30, high MOD intensity  $\geq$ 30), and Ki67 (C; low nuclear positivity <6%, high nuclear positivity  $\geq$ 6%). A, high H3K18Ac (>50% positivity) was significantly associated with an increased risk of PSA relapse (log rank statistic = 6.49,  $P = 0.011$ ). B, high H3K4diMe ( $\geq$ 30 MOD units) was significantly associated with an increased risk of PSA relapse (log rank statistic = 9.36,  $P = 0.002$ ). C, high Ki67 immunostaining ( $\geq$ 6% positivity) was significantly associated with an increased risk of PSA relapse (log rank statistic = 8.25,  $P = 0.004$ ).

(MOD), and total amount of staining (MIOD). There was a marked difference between H3K18Ac visual and VIA percentage of positivity frequency distributions, with the latter resulting in a more normal distribution (Supplementary Fig. S2A-B). In contrast, the frequency distributions of H3K18Ac MOD and MIOD are similar to each other but differ from percentage of positivity (Supplementary Fig. S2C-D). In contrast to H3K18Ac, the frequency distributions for H3K4diMe visual and

VIA positivity are very similar, whereas both MOD and MIOD frequency distributions are similar to each other but again differ from percentage of positivity (Supplementary Fig. S3A-D). The frequency distributions for H3K4diMe percentage of positivity are skewed to the right whereas for MOD and MIOD they are skewed to the left (Supplementary Fig. S3A-D).

H3K18Ac and H3K4diMe VIA positivity were not significantly correlated with any of the clinicopathologic

variables assessed (data not shown) but were significantly correlated with each other (Spearman correlation coefficient,  $r = 0.271$ ,  $P < 0.001$ ). H3K18Ac VIA positivity (Spearman correlation coefficient,  $r = 0.208$ ,  $P = 0.001$ ) but not H3K4diMe VIA positivity (Spearman correlation coefficient,  $r = 0.042$ ,  $P = 0.485$ ) was significantly correlated with the proliferation marker, Ki67 (median positive nuclei was 2%; range, 0-15%).

### H3K18Ac and H3K4diMe levels are associated with relapse-free survival

The only measure of H3K18Ac immunostaining that was significantly associated with relapse-free survival was H3K18Ac VIA positivity, either as a continuous variable ( $P = 0.043$ ) or when dichotomized using 50% positive nuclear area as a cutpoint ( $P = 0.012$ ; Table 1). Examples of prostate tumors with low and high H3K18Ac VIA positivity are shown in Fig. 1A. Similarly, the only immunostaining measure that was significant for H3K4diMe was MOD intensity as a continuous variable ( $P = 0.051$ ) and when dichotomized using 30 MOD units as a cutpoint ( $P = 0.019$ ; Table 1). Examples of prostate tumor tissues with comparable levels of H3K4diMe positivity (72.90% and 72.92%), but different levels of MOD (low = 19.19 units and high = 33.43 units), are shown in Fig. 1B. Age at diagnosis and clinical stage were not significantly associated with relapse-free survival (Table 1). All other significant variables are shown in Table 1. Univariate Cox regression analysis indicated that Ki67 status was significantly associated with relapse-free survival when assessed as a continuous variable ( $P = 0.011$ ) and when dichotomized into low (<6%) and high ( $\geq 6\%$ ) percentage of positive cells ( $P = 0.005$ ; Table 1; Fig. 1C).

Kaplan-Meier analysis showed that high H3K18Ac (VIA % nuclear area  $\geq 50\%$ ), high H3K4diMe (MOD intensity  $>30$ ), or high Ki67 (% positive nuclei,  $\geq 6\%$ ) immunostaining were significantly associated with an increased risk of relapse (Fig. 1A-C). When the cohort was divided on the basis of Gleason score, the relationship between high H3K18Ac levels and PSA relapse was only observed in patients with low Gleason score (i.e.,  $<7$ ; Supplementary Fig. S4A-B), as per the previous study (17). However, in contrast high H3K4diMe MOD levels were significantly associated with PSA relapse in patients with either low or high Gleason score (Supplementary Fig. S4C-D).

### H3K18Ac and H3K4diMe levels are independent predictors of PSA relapse

Multivariate Cox regression analysis indicated that preoperative PSA, Gleason score, Ki67 (% positive nuclei), H3K18Ac (VIA % positive nuclear area), and H3K4diMe (MOD intensity) were the only independent predictors of tumor recurrence following radical prostatectomy (Table 2). High levels of H3K18Ac and H3K4diMe were associated with a 1.71-fold and 1.80-fold increased risk of recurrence, respectively ( $P < 0.0001$  and

**Table 1.** Univariate Cox regression analysis of relapse-free survival in patients after radical prostatectomy

Variable	Relative risk (95% confidence interval)	P
Age at diagnosis ( $n = 279$ )	1.00 (0.97-1.03)	0.881
Clinical stage ( $n = 278$ )*	1.40 (0.93-2.11)	0.114
Pathologic stage ( $n = 279$ ) <sup>†</sup>	2.59 (1.75-3.84)	<b>&lt;0.0001</b>
Preoperative PSA ( $n = 263$ ) <sup>‡</sup>	1.78 (1.22-2.62)	<b>0.003</b>
Gleason score ( $n = 279$ ) <sup>§</sup>	2.58 (1.76-3.80)	<b>&lt;0.0001</b>
Margins ( $n = 279$ )	1.82 (1.24-2.68)	<b>0.002</b>
Seminal vesicle involvement ( $n = 279$ )	2.24 (1.52-3.30)	<b>&lt;0.0001</b>
Extracapsular extension ( $n = 279$ )	2.30 (1.56-3.39)	<b>&lt;0.0001</b>
Ki67 ( $n = 277$ ) <sup>  </sup>	1.08 (1.01-1.15)	<b>0.011</b>
Ki67 ( $n = 277$ ) <sup>¶</sup>	1.94 (1.22-3.07)	<b>0.005</b>
H3K18Ac POS ( $n = 279$ ) <sup>**</sup>	1.01 (1.00-1.02)	<b>0.043</b>
H3K18Ac POS ( $n = 279$ ) <sup>††</sup>	1.73 (1.13-2.64)	<b>0.012</b>
H3K18Ac MIOD ( $n = 279$ ) <sup>‡‡</sup>	1.02 (0.99-1.04)	0.167
H3K18Ac MOD ( $n = 279$ ) <sup>§§</sup>	1.00 (0.98-1.02)	0.734
H3K4diMe POS ( $n = 279$ ) <sup>   </sup>	1.00 (0.99-1.01)	0.939
H3K4diMe MIOD ( $n = 279$ ) <sup>¶¶</sup>	1.01 (0.99-1.02)	0.443
H3K4diMe MOD ( $n = 279$ ) <sup>***</sup>	1.02 (1.00-1.03)	0.051
H3K4diMe MOD ( $n = 279$ ) <sup>†††</sup>	1.56 (1.24-2.66)	<b>0.019</b>

NOTE: All statistical analyses (footnotes || to †††) were done with the highest core value present for each cancer case.

\*Clinical stage cT<sub>1</sub> and cT<sub>2</sub> (also includes 7 cases cT<sub>3</sub>).

†Pathologic stage pT<sub>2</sub> and pT<sub>3</sub>.

‡Gleason score  $<7$  vs.  $\geq 7$ .

§Preoperative serum PSA level (ng/mL) dichotomized by cutpoint  $<10.0$  vs.  $\geq 10.0$ .

||Ki67 (% positive cells) as a continuous variable.

¶Ki67 (% positive cells) dichotomized by low (<6% positive cells) vs. high ( $\geq 6\%$  positive cells).

\*\*H3K18Ac level (% positive nuclear area) as a continuous variable as measured by VIA.

††H3K18Ac level (% positive nuclear area) dichotomized by low (<50% nuclear area) vs. high ( $\geq 50\%$  nuclear area) as measured by VIA.

‡‡H3K18Ac MIOD total amount of staining as a continuous variable as measured by VIA.

§§H3K18Ac MOD intensity of staining as a continuous variable as measured by VIA.

|||H3K4diMe level (% positive nuclear area) as a continuous variable as measured by VIA.

¶¶H3K4diMe MIOD total amount of staining as a continuous variable as measured by VIA.

\*\*\*H3K4diMe MOD intensity of staining as a continuous variable as measured by VIA.

†††H3K4diMe MOD intensity of staining dichotomized by low (<30 MOD) vs. high ( $\geq 30$  MOD) as measured by VIA.

**Table 2. Multivariate Cox regression analyses****(A) Multivariate Cox regression analysis of relapse-free survival in patients treated with radical prostatectomy (all variables significant in univariate analysis,  $n = 236$ )**

Variable	Relative risk (95% confidence interval)	<i>P</i>
Pathologic stage*	2.08 (0.66-6.57)	0.210
PSA <sup>†</sup>	1.50 (0.98-2.29)	0.060
Gleason score <sup>‡</sup>	1.61 (1.01-2.57)	<b>0.047</b>
Seminal vesicle involvement	1.53 (0.84-2.82)	0.163
Margins	1.12 (0.72-1.84)	0.640
Extracapsular extension	0.64 (0.21-1.92)	0.423
Ki67 <sup>§</sup>	1.61 (0.94-2.68)	0.072
H3K18Ac POS <sup>  </sup>	1.72 (1.07-2.76)	<b>0.025</b>
H3K4diMe MOD <sup>¶</sup>	1.99 (1.30-3.06)	<b>0.002</b>

**(B) Multivariate Cox regression analysis of relapse-free survival in patients treated with radical prostatectomy (all independent variables,  $n = 254$ )**

PSA <sup>†</sup>	1.63 (1.09-2.43)	<b>0.017</b>
Gleason score <sup>‡</sup>	2.19 (1.46-3.29)	<b>&lt;0.0001</b>
Ki67 <sup>§</sup>	1.92 (1.18-3.11)	<b>&lt;0.0001</b>
H3K18Ac POS <sup>  </sup>	1.71 (1.08-2.69)	<b>&lt;0.0001</b>
H3K4diMe MOD <sup>¶</sup>	1.80 (1.19-2.74)	<b>0.006</b>

**(C) Multivariate analysis with histone score ( $n = 254$ )**

PSA <sup>†</sup>	1.60 (1.09-2.43)	<b>0.023</b>
Gleason score <sup>‡</sup>	2.18 (1.46-3.29)	<b>&lt;0.0001</b>
Ki67 <sup>§</sup>	1.83 (1.18-3.11)	<b>0.017</b>
Histone score**		
Score 0	1.00	—
Score 1	1.50 (0.89-2.52)	0.129
Score 2	1.13 (0.42-3.01)	0.823
Score 3	3.00 (1.73-5.31)	<b>&lt;0.0001</b>

\*Pathologic stage pT<sub>2</sub> and pT<sub>3</sub>.<sup>†</sup>Preoperative serum PSA level (ng/mL) dichotomized by cutpoint <10.0 vs. ≥10.0.<sup>‡</sup>Gleason score <7 vs. ≥7.<sup>§</sup>Ki67 (% positive cells) dichotomized by low (<6% positive cells) vs. high (≥6% positive cells).<sup>||</sup>H3K18Ac level (% positive nuclear area) dichotomized by low (<50% nuclear area) vs. high (≥50% nuclear area) as measured by VIA.<sup>¶</sup>H3K4diMe MOD intensity of staining dichotomized by low (<30 MOD) vs. high (≥30 MOD) as measured by VIA.

\*\*Histone score: score 0 = H3K18Ac % positive nuclear area &lt;50, H3K4diMe MOD intensity of staining &lt;30. Score 1 = H3K18Ac % positive nuclear area ≥50, H3K4diMe MOD intensity of staining &lt;30. Score 2 = H3K18Ac % positive nuclear area &lt;50, H3K4diMe MOD intensity of staining ≥30. Score 3 = H3K18Ac % positive nuclear area ≥50, H3K4diMe MOD intensity of staining ≥30.

$P = 0.006$ ). High levels of Ki67 were associated with a 1.92-fold increased risk ( $P < 0.0001$ ; Table 2).

**Combining H3K18Ac and H3K4diMe improves the prediction of tumor recurrence**

Combining H3K18Ac (VIA % positive nuclear area) and H3K4diMe (MOD intensity) to generate a histone score enabled patients to be stratified into four groups with the following predicted 5-year relapse-free survival rates: 77.2%, 71.7%, 81.3%, or 52.6% for a score of 0, 1, 2, or 3, respectively (Fig. 2). Patients with both high H3K18Ac positive nuclear area and high H3K4diMe MOD had the shortest time to relapse and the highest PSA failure rate (score 3; 63% of patients, 34 of 54; Fig. 2). The PSA failure rates between the four groups were statistically different (log rank statistic = 18.39,  $P < 0.0001$ ; Fig. 2). When the histone score index was analyzed with PSA, Gleason score, and Ki67 in a multivariate analysis, high levels of both histone modifications (histone score = 3) identified a subgroup of patients with an even greater risk of relapse (3-fold,  $P < 0.0001$ ) compared with preoperative PSA (1.6-fold,  $P < 0.023$ ) or Gleason score (2.2-fold,  $P < 0.0001$ ; Table 2C).

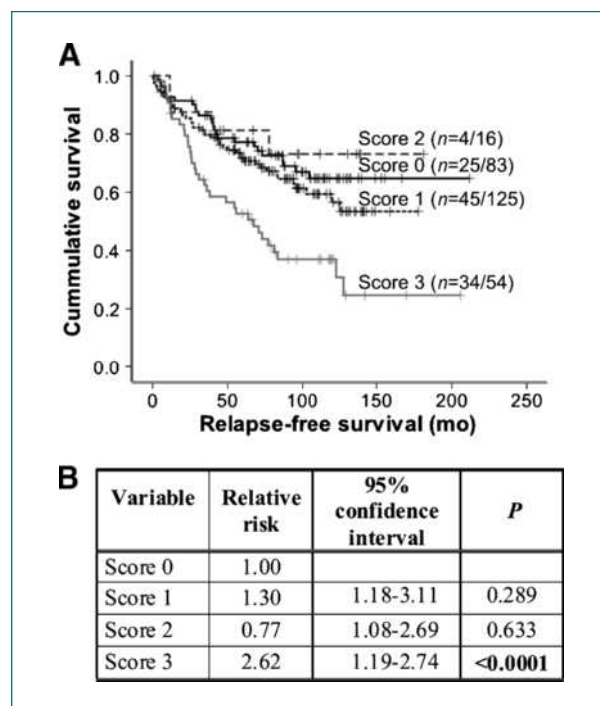


**Figure 2.** Kaplan-Meier product limit plots and Cox regression analysis of histone score. A, combinations of the two histone markers to generate a score such that score 0 = H3K18Ac positive nuclear area <50%, H3K4diMe MOD intensity <30; score 1 = H3K18Ac positive nuclear area ≥50%, H3K4diMe MOD intensity <30; score 2 = H3K18Ac positive nuclear area <50%, H3K4diMe MOD intensity ≥30; and score 3 = H3K18Ac positive nuclear area ≥50%, H3K4diMe MOD intensity ≥30. Patients with high levels of both histones (score 3) were at an increased risk of PSA relapse (log rank statistic = 18.39,  $P < 0.0001$ ). B, patients with a histone score of 3 had a 2.62 increased risk of relapse when compared with patients with a histone score of 0 ( $P < 0.0001$ ).

### Identification of a candidate epigenetic gene signature involved in prostate tumorigenesis

As specific global histone modifications were significantly associated with disease relapse, we assessed whether the genes regulating these modifications are altered in prostate cancer progression. We examined the expression of 74 epigenetic genes (26), including those involved in DNA methylation (DNMT), histone acetylation, histone deacetylation (HDAC), histone methylation (HMT) and histone demethylation, in a previously generated Affymetrix U95 prostate cancer progression microarray data set (refs. 31, 32; Supplementary Table S2 and Supplementary Fig. S5). In the primary tumors, we identified that 19 of the 74 epigenetic genes exhibited significantly different mean levels of expression in relapse-free patient samples compared with those from patients that subsequently underwent biochemical recurrence (Fig. 3A and C; Supplementary Table S2). Twenty-one genes were differentially expressed between primary and metastatic prostate lesions (Fig. 3B-C; Supplementary Table S2). Epigenetic genes identified that have been previously associated with prostate cancer included *EZH2*, a histone methyltransferase that methylates H3K27, which is expressed at a markedly higher level in the metastatic prostate lesions compared with the primary tumors (Fig. 3B; Supplementary Table S2). *EZH2* has previously been shown to predict biochemical recurrence in prostate cancer (36-38). Similarly, the DNA methyltransferases *DNMT1*, *DNMT3A*, and *DNMT3B* were significantly expressed at higher levels in metastases compared with the primary tumors (Fig. 3B; Supplementary Table S2), and have previously been shown to be upregulated in prostate cancer when compared with benign prostate tissue (39-41). The histone acetyltransferases *CREBBP* and *EP300*, the histone methyltransferase *CARM1*, and several HDACs previously implicated in prostate tumorigenesis (42-51), were also expressed at significantly higher levels in metastatic lesions (Fig. 3B).

Figure 3C illustrates the overlap between genes significantly altered in primary tumors with and without biochemical recurrence, and those altered between primary and metastatic tumors, and highlights a candidate epigenetic signature consisting of six genes associated with prostate cancer progression. *DNMT3A*, *MLL2*, *NSD1*, and *MLL3* were significantly downregulated and *MBD4* and *SRCAP* upregulated in the primary prostate cancer samples with biochemical recurrence when compared with the primary samples without recurrence (Fig. 3A). In the metastatic samples, these same six genes were also significantly altered, with *DNMT3A*, *MLL2*, *NSD1*, *MBD4*, and *MLL3* upregulated and *SRCAP* downregulated when compared with the primary prostate tumors (Fig. 3B). The epigenetic gene changes observed in our cohort comparing primary and metastatic prostate tumors were also verified in microarray data sets available in ONCOMINE (52) comparing nonmalignant and prostate cancer tissues (data not shown).

### An epigenetic gene signature that predicts nonmalignant from prostate tumor tissue

In an independent cohort of 22 matched nonmalignant and prostate tumor samples, only *MLL3* and *EZH2*, the latter used as a positive control, were significantly altered between the nonmalignant and tumor samples (Fig. 4A-B; Wilcoxon signed rank test,  $P = 0.005$  and  $P = 0.044$ , respectively). As expected, for *EZH2*, the Gleason score 9 sample had the highest fold change. It is not surprising that the other epigenetic genes were not significantly altered between the matched nonmalignant and tumor cases because the tumor specimens had not been microdissected and may have had extensive nonmalignant tissue present. However, the combination of all six epigenetic genes (*MLL3*, *MLL2*, *NSD1*, *DNMT3A*, *MBD4*, and *SRCAP*) in a multivariate ANOVA significantly differentiated nonmalignant from tumor tissue (Fig. 4H;  $P = 0.006$ ).

### Discussion

The clinical significance of epigenetic alterations in prostate carcinogenesis has only recently begun to be elucidated. It has previously been shown that levels of two histone modifications, H3K18Ac and H3K4diMe, in combination could predict prostate cancer recurrence, but only when confined to low Gleason score tumors (17). In this study, we report that H3K18Ac and H3K4diMe independently predict prostate cancer relapse following radical prostatectomy, with high levels of either marker being associated with a poor outcome. Patients with high levels of both histone modifications have a 3-fold increased risk of tumor recurrence compared with patients with low levels of both markers. Notably, the combined histone score was better at predicting patients with a poor outcome compared with either preoperative PSA or Gleason score.

When the patient cohort in our study was stratified according to Gleason score, H3K18Ac was a significant predictor of relapse for low-grade patients only, whereas H3K4diMe levels were a significant predictor in patient groups with low or high Gleason scores. These findings are in contrast to those of Seligson et al. (17), who showed that high levels of H3K18Ac and H3K4diMe are associated with a better prognosis in patients with low Gleason score only. Paradoxically, Seligson et al. (17) also reported that increased H3K18Ac and H3K4diMe levels were positively correlated with increasing tumor grade, consistent with our study in which higher levels of each histone modification were associated with a poor outcome.

A recent study investigating esophageal squamous cell carcinoma (53) found that high levels of H3K18Ac or H3K4diMe are associated with a poor prognosis, whereas other studies in breast, lung, prostate, and kidney cancers have shown the opposite relationship (10, 17, 20, 28). The differences between these studies may reflect different methods for assessing immunostaining levels of

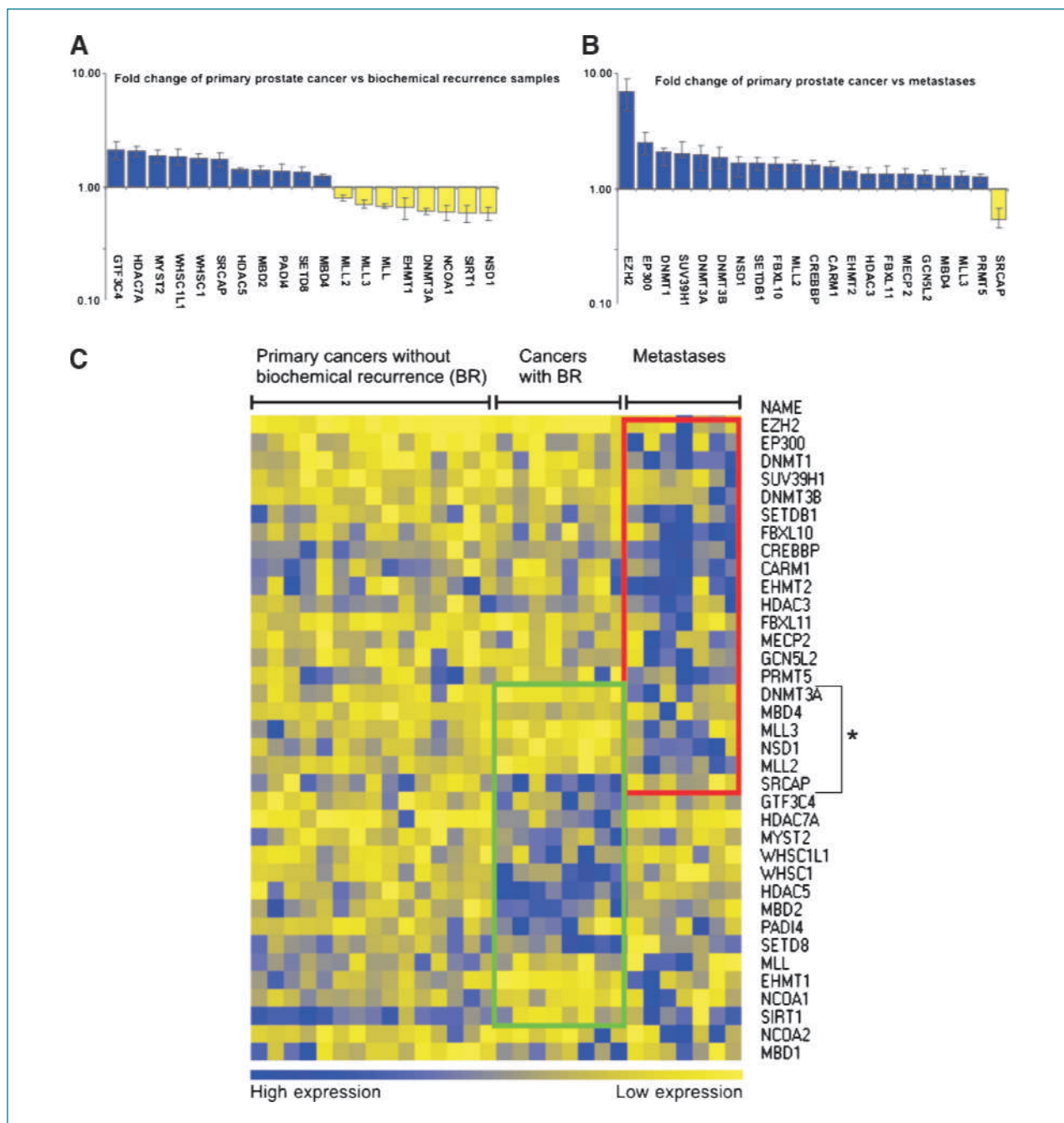


**Figure 3.** Microarray epigenetic gene expression in primary and metastatic prostate cancers. A, nineteen epigenetic genes were identified that were significantly altered between primary prostate cancer samples with and without biochemical recurrence. Average fold change (+SEM) between the primary versus biochemical recurrence samples from significant probes ( $P < 0.05$ ). Gene probes are ranked by fold change. B, twenty-one epigenetic genes were significantly altered between primary and metastatic prostate cancer samples. Average fold change (+SEM) between the primary versus metastatic samples from significant probes ( $P < 0.05$ ). Gene probes are ranked by fold change. C, a heat map was generated using Heatmap Builder version 1.0. The green box indicates the genes which had a significantly different expression level between the primary prostate cancer samples with and without biochemical recurrence. The red box indicates the genes which had a significantly different expression level between the primary tumors and the metastases. \*, the six overlapping genes between the green and red box which constitutes the candidate epigenetic gene signature.

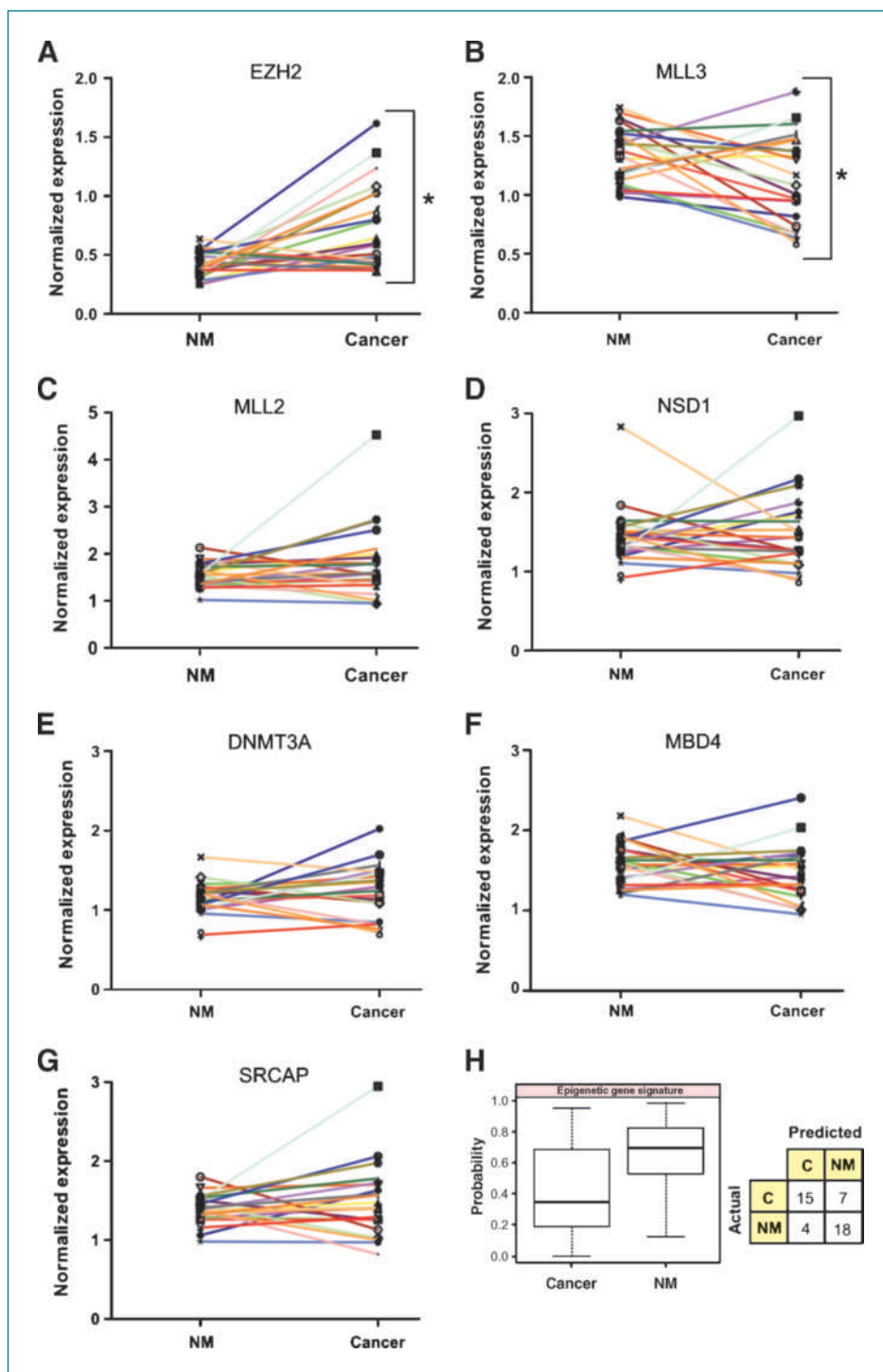
these histone modifications. A strength of the present study is that we used VIA, which provides an objective, reproducible, and unbiased assessment of immunostaining (24, 25, 29). VIA calculates three independent

measures of immunoperoxidase staining: positivity (% positive nuclear area), the intensity of these positive cells as mean integrated optical density in the tissue area (MIOD, concentration), or mean optical density (MOD,

intensity). Different immunohistochemical quantitation methods may influence both the pattern and level of staining. For example, whereas the frequency distribution of H3K18Ac positivity assessed by visual scoring is markedly skewed to the right and is similar to that reported previously (17), a normal frequency distribution was

observed for H3K18Ac positivity as determined by VIA. The distinct difference in the H3K18Ac immunostaining frequency distributions generated by the two assessment methodologies (Supplementary Fig. S2) may account for H3K18Ac positivity, as determined by VIA but not by visual assessment, being a significant predictor of disease

**Figure 4.** The epigenetic gene signature predicts nonmalignant from tumor prostate tissue. TaqMan gene expression assays for (A) *EZH2*, a positive control, and the candidate epigenetic gene signature (B) *MLL3*, (C) *MLL2*, (D) *NSD1*, (E) *DNMT3A*, (F) *MBD4*, and (G) *SRCAP* indicated that only (A) *EZH2* and (B) *MLL3* were significantly altered (Wilcoxon signed rank test;  $P = 0.0052$  and  $P = 0.0441$ , respectively) between nonmalignant and tumor tissue in 22 matched prostate tumor cases. Each line represents a matched nonmalignant/tumor prostate case. Using multivariate ANOVA (H) for *MLL3*, *MLL2*, *NSD1*, *DNMT3A*, *MBD4*, and *SRCAP* combined indicated that the epigenetic gene signature was able to significantly predict nonmalignant and tumor tissue ( $P = 0.0063$ ). All gene expression levels were normalized to the reference genes *GAPDH*, *GUSB*, and *HPRT1*.



relapse. The likely explanation for the differences in frequency distribution between the two methods is that VIA assesses the area of brown staining within each nucleus to record the mean nuclear positive area, thereby providing a different measure of immunostaining (i.e., area of positive nuclear staining) compared with visual scoring (number of positive nuclei).

In this study, we found that the mean intensity of H3K4diMe expression per nucleus (MOD), but not the percentage of positivity or total amount of staining (MIOD), is an independent predictor of prostate cancer outcome. Although the majority of patients have high levels of H3K4diMe in their prostate tumors, the most important parameter biologically seems to be the level of expression (i.e., intensity) within individual nuclei (Supplementary Fig. S3).

Although the exact mechanisms whereby histone modifications are altered during carcinogenesis are unknown, it is possible that, similar to DNA methylation, an increase and decrease in different histone modifications might occur concurrently during cancer progression, resulting in overexpression as well as silencing of genes. For instance, the epigenetic genes identified as significantly altered in prostate tumorigenesis in our study was comprised of several histone acetyltransferases as well as histone deacetylases. In addition, differential expression changes of specific histone modifications may also occur during prostate cancer progression. Recently, H3K4monoMe, H3K9diMe, H3K9triMe, H3Ac, and H4Ac were shown to be significantly reduced in prostate tumors when compared with nonmalignant tissue, and H3Ac and H3K9diMe levels were able to discriminate prostate cancer from nonmalignant tissue (54). Indeed, the global levels of histone modifications H3K4monoMe, H3K9monoMe, H3K9diMe, H3K9triMe, H3Ac, and H4Ac, but not H3K4diMe and H3K4triMe, were reduced in localized prostate cancer compared with nonmalignant tissues (54). However, when localized and hormone-refractory prostate cancer was compared, an increase in the histone modifications was observed (54). Remarkably, five out of six genes identified in our epigenetic gene signature were differentially expressed at different stages of prostate cancer (primary cancer versus biochemical recurrence or primary cancer versus metastases) providing further evidence of the differential expression changes of global histone modifications during prostate cancer progression.

Although global changes of a specific histone modification do not necessarily equate with alterations in the expression of specific genes, the expression patterns of specific histone modifications and histone-modifying enzymes can differentiate tumor samples from normal tissue and cluster tumor samples according to cell type (54-56). In this study, we provide evidence that in addition to the histone modifications, histone-modifying enzymes or epigenetic genes also undergo alterations in expression during prostate cancer progression. A putative epigenetic gene signature including genes involved

in DNA methylation (*DNMT3A* and *MBD4*), histone methyltransferases (*MLL2*, *MLL3*, and *NSD1*), and the histone acetyltransferase (*SRCAP*) was identified. Whereas *DNMT3A* and *MBD4* have previously been found to be altered in prostate cancer (39, 57), this is not the case for *MLL2*, *MLL3*, *SRCAP*, and *NSD1* (reviewed in ref. 26). Most importantly, the majority of these epigenetic genes regulate specific histone modifications such as H3K4 methylation (i.e., *MLL* family members) and H3K18 acetylation (i.e., *CBP*, *EP300*, and *GCN5L2*), which is in accordance with our findings that H3K18Ac and H3K4diMe are independent predictors of prostate cancer recurrence. The epigenetic genes *SUV39H1*, *SETDB1*, and *EHMT1*, involved in the methylation of the H3K9 residue, were also identified as being altered with prostate cancer progression, consistent with the findings of Ellinger et al. (54), who showed that H3K9diMe is predictive of low-grade prostate cancer. Collectively, these results suggest the major role of histone methylation throughout prostate cancer progression.

Consistent with a recent study (55) investigating epigenetic gene expression changes between primary prostate tumors and benign samples, 13 of the 21 genes identified in our microarray data mining analysis as being significantly altered between primary and metastatic prostate cancer samples were also identified by Ke et al. (55); and of these, 69% (9 of 13) were involved in DNA methylation and histone methylation. Whereas most studies that endeavor to develop epigenetic therapies have focused on DNA methyltransferase inhibitors (DNMTi) and histone deacetylase inhibitors (HDACi), our results together with Ke et al. (55) highlight the importance of HMTs in prostate tumorigenesis, and that histone methylation inhibitors (HMTi) are potential therapeutic targets for prostate cancer. Moreover, identification of DNMT/MBDs and histone acetylations as the second most significantly altered category of epigenetic genes suggests the potential for a combination therapy for prostate cancer. To date, a treatment option with a HMTi combined with a DNMTi or HDACi for the treatment of prostate cancer has not been investigated, but this will be increasingly plausible with the development of new HMTi and more stable and less cytotoxic DNMTi alternatives.

In summary, we have identified the prognostic potential of histone modifications in prostate cancer. We also report an epigenetic gene signature associated with prostate tumorigenesis, suggesting that targeting the epigenetic enzymes specifically involved in prostate cancer may enhance therapeutic response to epigenetic therapies. Testing for aberrant expression of epigenetic genes, such as those identified in this study, may be used to identify patients who are likely to respond to epigenetic therapies, monitor response to these therapies, and predict patient outcome.

#### Disclosure of Potential Conflicts of Interest

No potential conflicts of interest were disclosed.

## Acknowledgments

The authors thank Dr. Andrew Sakko for assistance with data analysis. We also thank Anne-Maree Haynes and Ruth Pe Benito for their assistance with the management of the patient database and tissue bank in relation to the SVCPCG cohort. We are grateful to the study participants, as well as the urologists, nurses, and histopathologists who kindly assisted in the recruitment and collection of patient information and pathology reports. The authors acknowledge in particular the excellent technical contributions of the following people: at Hanson Institute Adelaide, Helen Hughes; at QUT Brisbane, Pam Saunders; at Monash Institute Melbourne, Brian Golat and Ruth Patterson; at Garvan Institute Sydney, Ruth Pe Benito. Thank you also to Dr. Luke Selth for reading the manuscript.

## Grant Support

Cancer Council of SA (Fellowship to T. Bianco-Miotto and L.M. Butler); National Health and Medical Research Council (Career Development

Award, G. Buchanan); University of Adelaide Medical Endowment Funds (Hilda Farmer Research Fellowship, C. Ricciardelli); University of Adelaide (Postgraduate International Scholarship, K. Chiam); the National Health and Medical Research Council (NHMRC, Project Grant No. 349457, D.J. Horsfall, C. Ricciardelli, V.R. Marshall, and W.D. Tilley; no. 453662, W.D. Tilley, L.M. Butler, and V.R. Marshall; no. 627185, W.D. Tilley, L.M. Butler, H.I. Scher, and T. Bianco-Miotto); NHMRC (Enabling Grant No. 290456 to the Australian Prostate Cancer BioResource—J.A. Clements, G.P. Risbridger, R.L. Sutherland, and W.D. Tilley); the U.S. Department of Defense (W81XWH-04-1-0017, W.D. Tilley); the Prostate Cancer Foundation of Australia (G. Buchanan; ID no. Y102), Cancer Institute NSW & RT Hall Trust.

The costs of publication of this article were defrayed in part by the payment of page charges. This article must therefore be hereby marked *advertisement* in accordance with 18 U.S.C. Section 1734 solely to indicate this fact.

Received 05/26/2010; revised 07/08/2010; accepted 08/05/2010; published OnlineFirst 09/14/2010.

## References

1. Esteller M. Cancer epigenomics: DNA methylomes and histone-modification maps. *Nat Rev Genet* 2007;8:286–98.
2. Dobosy JR, Roberts JL, Fu VX, Jarrard DF. The expanding role of epigenetics in the development, diagnosis and treatment of prostate cancer and benign prostatic hyperplasia. *J Urol* 2007;177:822–31.
3. Hake SB, Xiao A, Allis CD. Linking the epigenetic 'language' of covalent histone modifications to cancer. *Br J Cancer* 2004;90:761–9.
4. Szyf M. DNA methylation and demethylation as targets for anticancer therapy. *Biochemistry (Mosc)* 2005;70:533–49.
5. Szyf M, Pakneshan P, Rabbani SA. DNA demethylation and cancer: therapeutic implications. *Cancer Lett* 2004;211:133–43.
6. Baylín SB, Herman JG. DNA hypermethylation in tumorigenesis: epigenetics joins genetics. *Trends Genet* 2000;16:168–74.
7. Esteller M. Aberrant DNA methylation as a cancer-inducing mechanism. *Annu Rev Pharmacol Toxicol* 2005;45:629–56.
8. Miyamoto K, Ushijima T. Diagnostic and therapeutic applications of epigenetics. *Jpn J Clin Oncol* 2005;35:293–301.
9. Park YS, Jin MY, Kim YJ, Yook JH, Kim BS, Jang SJ. The global histone modification pattern correlates with cancer recurrence and overall survival in gastric adenocarcinoma. *Ann Surg Oncol* 2008;15:1968–76.
10. Barlesi F, Giaccone G, Gallegos-Ruiz MI, et al. Global histone modifications predict prognosis of resected non small-cell lung cancer. *J Clin Oncol* 2007;25:4358–64.
11. Fraga MF, Ballestar E, Villar-Garea A, et al. Loss of acetylation at Lys16 and trimethylation at Lys20 of histone H4 is a common hallmark of human cancer. *Nat Genet* 2005;37:391–400.
12. Tryndyak VP, Kovalchuk O, Pogribny IP. Loss of DNA methylation and histone H4 lysine 20 trimethylation in human breast cancer cells is associated with aberrant expression of DNA methyltransferase 1, Suv4-20h2 histone methyltransferase and methyl-binding proteins. *Cancer Biol Ther* 2006;5:65–70.
13. Kondo Y, Shen L, Cheng AS, et al. Gene silencing in cancer by histone H3 lysine 27 trimethylation independent of promoter DNA methylation. *Nat Genet* 2008;40:741–50.
14. Wei Y, Xia W, Zhang Z, et al. Loss of trimethylation at lysine 27 of histone H3 is a predictor of poor outcome in breast, ovarian, and pancreatic cancers. *Mol Carcinog* 2008;47:701–6.
15. Mohamed MA, Greif PA, Diamond J, et al. Epigenetic events, remodeling enzymes and their relationship to chromatin organization in prostatic intraepithelial neoplasia and prostatic adenocarcinoma. *BJU Int* 2007;99:908–15.
16. Yegnasubramanian S, Haffner MC, Zhang Y, et al. DNA hypomethylation arises later in prostate cancer progression than CpG island hypermethylation and contributes to metastatic tumor heterogeneity. *Cancer Res* 2008;68:8954–67.
17. Seligson DB, Horvath S, Shi T, et al. Global histone modification patterns predict risk of prostate cancer recurrence. *Nature* 2005;435:1262–6.
18. Kouzarides T. Chromatin modifications and their function. *Cell* 2007;128:693–705.
19. Esteller M. Epigenetics in cancer. *N Engl J Med* 2008;358:1148–59.
20. Seligson DB, Horvath S, McBrien MA, et al. Global levels of histone modifications predict prognosis in different cancers. *Am J Pathol* 2009;174:1619–28.
21. Henshall SM, Horvath LG, Quinn DI, et al. Zinc- $\alpha$ -2-glycoprotein expression as a predictor of metastatic prostate cancer following radical prostatectomy. *J Natl Cancer Inst* 2006;98:1420–4.
22. Sakko AJ, Butler MS, Byers S, et al. Immunohistochemical level of unsulfated chondroitin disaccharides in the cancer stroma is an independent predictor of prostate cancer relapse. *Cancer Epidemiol Biomarkers Prev* 2008;17:2488–97.
23. Horvath LG, Henshall SM, Lee CS, et al. Lower levels of nuclear  $\beta$ -catenin predict for a poorer prognosis in localized prostate cancer. *Int J Cancer* 2005;113:415–22.
24. Horsfall DJ, Jarvis LR, Grimbaldeston MA, Tilley WD, Orell SR. Immunocytochemical assay for oestrogen receptor in fine needle aspirates of breast cancer by video image analysis. *Br J Cancer* 1989;59:129–34.
25. Tilley WD, Lim-Tio SS, Horsfall DJ, Aspinall JO, Marshall VR, Skinner JM. Detection of discrete androgen receptor epitopes in prostate cancer by immunostaining: measurement by color video image analysis. *Cancer Res* 1994;54:4096–102.
26. Miremadi A, Oestergaard MZ, Pharoah PD, Caldas C. Cancer genetics of epigenetic genes. *Hum Mol Genet* 2007;16:R28–49.
27. Hermanek P. [1992 tumor classification/developments]. *Langenbecks Arch Chir Suppl Kongressbd* 1992:40–5.
28. Elsheikh SE, Green AR, Rakha EA, et al. Global histone modifications in breast cancer correlate with tumor phenotypes, prognostic factors, and patient outcome. *Cancer Res* 2009;69:3802–9.
29. Ricciardelli C, Choong CS, Buchanan G, et al. Androgen receptor levels in prostate cancer epithelial and peritumoral stromal cells identify non-organ confined disease. *Prostate* 2005;63:19–28.
30. Ricciardelli C, Jackson MW, Choong CS, et al. Elevated levels of HER-2/neu and androgen receptor in clinically localized prostate cancer identifies metastatic potential. *Prostate* 2008;68:830–8.
31. Buchanan G, Ricciardelli C, Harris JM, et al. Control of androgen receptor signaling in prostate cancer by the cochaperone small glutamine rich tetratricopeptide repeat containing protein  $\alpha$ . *Cancer Res* 2007;67:10087–96.
32. Holzbeierlein J, Lal P, LaTulippe E, et al. Gene expression analysis of human prostate carcinoma during hormonal therapy identifies androgen-responsive genes and mechanisms of therapy resistance. *Am J Pathol* 2004;164:217–27.
33. Spin JM, Nallamshetty S, Tabibiazar R, et al. Transcriptional profiling

- of *in vitro* smooth muscle cell differentiation identifies specific patterns of gene and pathway activation. *Physiol Genomics* 2004;19:292–302.
34. Lockwood CA, Ricciardelli C, Raymond WA, Seshadri R, McCaul K, Horsfall DJ. A simple index using video image analysis to predict disease outcome in primary breast cancer. *Int J Cancer* 1999;84:203–8.
  35. Ricciardelli C, Sakko AJ, Stahl J, Tilley WD, Marshall VR, Horsfall DJ. Prostatic chondroitin sulfate is increased in patients with metastatic disease but does not predict survival outcome. *Prostate* 2009;69:761–9.
  36. Varambally S, Dhanasekaran SM, Zhou M, et al. The polycomb group protein EZH2 is involved in progression of prostate cancer. *Nature* 2002;419:624–9.
  37. Bryant RJ, Cross NA, Eaton CL, Hamdy FC, Cunliffe VT. EZH2 promotes proliferation and invasiveness of prostate cancer cells. *Prostate* 2007;67:547–56.
  38. Rhodes DR, Sanda MG, Otte AP, Chinnaiyan AM, Rubin MA. Multiplex biomarker approach for determining risk of prostate-specific antigen-defined recurrence of prostate cancer. *J Natl Cancer Inst* 2003;95:661–8.
  39. Patra SK, Patra A, Zhao H, Dahiya R. DNA methyltransferase and demethylase in human prostate cancer. *Mol Carcinog* 2002;33:163–71.
  40. Hoffmann MJ, Engers R, Florl AR, Otte AP, Muller M, Schulz WA. Expression changes in EZH2, but not in BMI-1, SIRT1, DNMT1 or DNMT3B are associated with DNA methylation changes in prostate cancer. *Cancer Biol Ther* 2007;6:1403–12.
  41. Pritchard C, Mecham B, Dumpit R, et al. Conserved gene expression programs integrate mammalian prostate development and tumorigenesis. *Cancer Res* 2009;69:1739–47.
  42. Comuzzi B, Nemes C, Schmidt S, et al. The androgen receptor coactivator CBP is up-regulated following androgen withdrawal and is highly expressed in advanced prostate cancer. *J Pathol* 2004;204:159–66.
  43. Hong H, Kao C, Jeng MH, et al. Aberrant expression of CARM1, a transcriptional coactivator of androgen receptor, in the development of prostate carcinoma and androgen-independent status. *Cancer* 2004;101:83–9.
  44. Isharwal S, Miller MC, Marlow C, Makarov DV, Partin AW, Veltri RW. p300 (histone acetyltransferase) biomarker predicts prostate cancer biochemical recurrence and correlates with changes in epithelia nuclear size and shape. *Prostate* 2008;68:1097–104.
  45. Debes JD, Sebo TJ, Lohse CM, Murphy LM, Haugen DA, Tindall DJ. p300 in prostate cancer proliferation and progression. *Cancer Res* 2003;63:7638–40.
  46. Fu M, Rao M, Wang C, et al. Acetylation of androgen receptor enhances coactivator binding and promotes prostate cancer cell growth. *Mol Cell Biol* 2003;23:8563–75.
  47. Fu M, Wang C, Reutens AT, et al. p300 and p300/cAMP-response element-binding protein-associated factor acetylate the androgen receptor at sites governing hormone-dependent transactivation. *J Biol Chem* 2000;275:20853–60.
  48. Patra SK, Patra A, Dahiya R. Histone deacetylase and DNA methyltransferase in human prostate cancer. *Biochem Biophys Res Commun* 2001;287:705–13.
  49. Halkidou K, Cook S, Leung HY, Neal DE, Robson CN. Nuclear accumulation of histone deacetylase 4 (HDAC4) coincides with the loss of androgen sensitivity in hormone refractory cancer of the prostate. *Eur Urol* 2004;45:382–9, author reply 9.
  50. Halkidou K, Gaughan L, Cook S, Leung HY, Neal DE, Robson CN. Upregulation and nuclear recruitment of HDAC1 in hormone refractory prostate cancer. *Prostate* 2004;59:177–89.
  51. Weichert W, Roske A, Gekeler V, et al. Histone deacetylases 1, 2 and 3 are highly expressed in prostate cancer and HDAC2 expression is associated with shorter PSA relapse time after radical prostatectomy. *Br J Cancer* 2008;98:604–10.
  52. Rhodes DR, Yu J, Shanker K, et al. ONCOMINE: a cancer microarray database and integrated data-mining platform. *Neoplasia* 2004;6:1–6.
  53. Tzao C, Tung HJ, Jin JS, et al. Prognostic significance of global histone modifications in resected squamous cell carcinoma of the esophagus. *Mod Pathol* 2009;22:252–60.
  54. Ellinger J, Kahl P, von der Gathen J, et al. Global levels of histone modifications predict prostate cancer recurrence. *Prostate* 2010;70:61–9.
  55. Ke XS, Qu Y, Rostad K, et al. Genome-wide profiling of histone h3 lysine 4 and lysine 27 trimethylation reveals an epigenetic signature in prostate carcinogenesis. *PLoS One* 2009;4:e4687.
  56. Ozdag H, Teschendorff AE, Ahmed AA, et al. Differential expression of selected histone modifier genes in human solid cancers. *BMC Genomics* 2006;7:90.
  57. Pang ST, Weng WH, Flores-Morales A, et al. Cytogenetic and expression profiles associated with transformation to androgen-resistant prostate cancer. *Prostate* 2006;66:157–72.